[Reply] We appreciate your constructive comments on this manuscript. We revised the manuscript to fully address your comments and suggestions. Detailed point-by-point responses to your comments and related revisions are presented below. The original comments are in black, and our responses are in blue color.

1. The OCO-2 v10 MIP sampled a much wider set of aircraft data than those used in this study. In particular NOAA operates a light aircraft program that produces regular profiles of CO2 measurements over North America and Raratonga. These data should be well suited to the analysis conducted here due to the regular sampling frequency, nearly continuous coverage, and altitudes sampled. For some reason, of these timeseries stations, only the data from Dahlen, North Dakota (DND) and Marcellus, Pennsylvania (MRC) were included in Table 1 of the manuscript. In addition to these two sites, there are evaluation data in the OCO-2 MIP samples from timeseries over:
Briggsdale, Colorado - (CAR)
Offshore Cape May, New Jersey - (CMA)
Carbon in Arctic Reservoirs Vulnerability Experiment (CARVE) - (CRV)
Estevan Point, British Columbia - (ESP)
East Trout Lake, Saskatchewan - (ETL)
Homer, Illinois - (HIL)
INFLUX (Indianapolis Flux Experiment) - (INX)
Park Falls, Wisconsin - (LEF)
Offshore Portsmouth, New Hampshire (Isles of Shoals) - (NHA)
Poker Flat, Alaska - (PFA)
Rarotonga - (RTA)
Offshore Charleston, South Carolina - (SCA)
Southern Great Plains, Oklahoma - (SGP)
Offshore Corpus Christi, Texas - (TGC)
Trinidad Head, California - (THD)
West Branch, Iowa - (WBI)

[Reply] We appreciate your suggestions. In this study, only measurement data not assimilated in the LNLGIS experiment were utilized for analysis. Additionally, we required a minimum of 10 observations per month at each 1°x1° grid point to calculate error statistics. Consequently, many of the airborne measurement data in OCO-2 MIP datasets did not meet our analysis criteria. We re-evaluated the availability of the dataset and the list of data used (Table 1 of the revised manuscript; shown in Table R1) to include all airborne measurements that meet our standards at least once. Through this process, CAR, PFA, and SGP data were newly incorporated into the analysis, while data that did not meet the criteria, AOA and MRC, were excluded from the data list. The addition of these three data sets did not result in any noticeable changes in our results.

Table R1 Data description for each airborne measurement campaign.

Site code	Site name	Measurement campaign name	Measurement type	Data provider	ObsPack (*original*) dataset identifier	Reference
ACG	Alaska Coast Guard	NOAA/GML Aircraft Program	In situ	National Oceanic and Atmospheric Administration (NOAA) Global Monitoring Laboratory (GML)	http://doi.org/10.25925/20201204[a]	
ACT	Atmospheric Carbon and Transport – America (ACT-America)	ACT-America	In situ and flask	NASA Langley Research Center (NASA-LaRC), NOAA/GML	http://doi.org/10.25925/20201204[a] *https://doi.org/10.3334/ORNLDAAC/1593*	Baier et al. (2020) Wei et al. (2021)

AirCore NOAA	NOAA AirCore	NOAA AirCore Program	Balloon	NOAA/GML	No Obspack DOI[b] *https://doi.org/10.15138/6AV0-MY81*	Karion et al. (2010)
ALF	Alta Floresta		Flask	National Institute for Space Research (INPE)	http://dx.doi.org/10.25925/20181030[c] https://doi.org/10.1594/PANGAEA.926834	Gatti et al. (2023)
CAR	Briggsdale, Colorado		Flask	NOAA/GML	http://doi.org/10.25925/20210517[d]	Sweeney et al. (2015)
CON	Comprehensive Observation Network for TRace gases by AIrLiner (CONTRAIL)		In situ	National Institute for Environmental Studies (NIES), Meteorological Research Institute (MRI)	http://doi.org/10.25925/20201204[a] *https://doi.org/10.17595/20180208.001*	Machida et al. (2008)
CRV	Carbon in Arctic Reservoirs Vulnerability Experiment (CARVE)	Arctic-Boreal Vulnerability Experiment (ABoVE)	In situ	NOAA/GML	http://doi.org/10.25925/20201204[a] *https://doi.org/10.3334/ORNLDAAC/1582*	
GSFC	NASA Goddard Space Flight Center Aircraft Campaign		In situ	NASA Goddard Space Flight Center (NASA-GSFC)	http://doi.org/10.25925/20201204[a]	Kawa et al. (2018)
IAGOS	In-service Aircraft for a Global Observing System	Civil Aircraft for the Regular Investigation of the atmosphere Based on an Instrument Container (IAGOS-CARIBIC)	In situ	Karlsruhe Institute of Technology (IMK-ASF), Institute for Atmospheric and Environmental Sciences (IAU), Max Planck Institute for Biogeochemistry (MPI-BGC)	http://doi.org/10.25925/20201204[a]	Filges et al. (2015)
LARC	LARC - NASA Langley Research Center Aircraft Campaign	Korea-United States Air Quality Study	In situ	NASA-LaRC	http://doi.org/10.25925/20201204[a]	
MAN	Manaus		In situ	NOAA/GML	https://doi.org/10.25925/20210519[e]	
ORC	O2/N2 Ratio and CO2 Airborne Southern Ocean Study (ORCAS)		In situ	National Center for Atmospheric Research (NCAR)	http://doi.org/10.25925/20201204[a] *https://doi.org/10.5065/D6SB445X*	Stephens et al. (2018)
PAN	Pantanal, Mato Grosso do Sul		Flask	INPE	http://dx.doi.org/10.25925/20181030[c]	
PFA	Poker Flat, Alaska		Flask	NOAA/GML	http://doi.org/10.25925/20210517[d]	Sweeney et al. (2015)
RBA-B	Rio Branco		Flask	INPE	http://dx.doi.org/10.25925/20181030[c] *https://doi.org/10.1594/PANGAEA.926834*	Gatti et al. (2023)
SAN	Santarem		Flask	INPE	http://dx.doi.org/10.25925/20181030[c] *https://doi.org/10.1594/PANGAEA.926834*	Gatti et al. (2023)
SGP	Southern Great Plains, Oklahoma		Flask	The US Department of Energy (DOE)/Lawrence Berkeley National Laboratory (LBNL)	http://doi.org/10.25925/20210517[d]	Biraud et al. (2013)
SONGNEX2015	Shale Oil and Natural Gas Nexus 2015 (air campaign)		In situ	NOAA Chemical Sciences Laboratory (CSL)	http://doi.org/10.25925/20201204[a]	
TEF	Tefe		Flask	INPE	http://dx.doi.org/10.25925/20181030[c] *https://doi.org/10.1594/PANGAEA.926834*	Gatti et al. (2023)
TOM	Atmospheric Tomography Mission (ATom)		In situ	NOAA/GML, Harvard University	http://doi.org/10.25925/20201204[a] *https://doi.org/10.3334/ORNLDAAC/1581*	

[a]: obspack_co2_1_GLOBALVIEWplus_v6.1_2021-03-01 (Schuldt et al., 2021b)
[b]: obspack_co2_1_AirCore_v4.0_2020-12-28
[c]: obspack_co2_1_INPE_RESTRICTED_v2.0_2018-11-13 (NOAA Carbon Cycle Group ObsPack Team, 2018)
[d]: obspack_co2_1_NRT_v6.1.1_2021-05-17 (Schuldt et al., 2021a)
[e]: obspack_multi-species_1_manaus_profiles_v1.0_2021-05-20 (Miller et al., 2021)

2. This reviewer's experience with simulation of aircraft measurements is that model residuals are strongly affected by altitude and by season. The analysis here does not discriminate by either of these factors, except to choose an altitude range apparently chosen to minimize the effect of residuals closer to the surface. Should the model residuals have significant variability by these factors, the evaluation criteria would be affected and possibly dominated by those factors, which would confound the statistical conclusions of this work. I suggest that a factor analysis, possibly an analysis of variance, is needed to determine whether model residuals are driven by these factors.

[Reply] Based on the reviewer's suggestions, we conducted additional analyses to explore how our results vary seasonally and with changes in the chosen altitude range.

First, to isolate the seasonal impacts on the regional error statistics (e.g., RMSE, ERR_{TOT}, $h(err_{f_e})$, and $h(err_{f_t})$), it is essential that other factors influencing the error quantities, such as the number of observation points and observation coverage within each region, remain consistent across seasons. Among the seven regions analyzed, in East Asia, the CONTRAIL program has continuously conducted measurements over three years with routes repeated throughout all seasons. The total numbers of observed grid-points per month during the vegetation growing season (from May to October) and non-growing season for 2015–2017 are comparable, amounting to 404 and 428, respectively. Furthermore, the area most sensitive to airborne measurements exhibit similar spatial patterns in both seasons, encompassing the northeast part of China, the Korean Peninsula, and Japan (Figure R1). By focusing on this region, we examined how the error quantities vary by seasons.

For the period 2015-2017, the regional averages of both RMSE and ERR_{TOT} exhibit, on average, 14% and 11% higher values during the non-growing season compared to the growing season (Figure R2). In contrast, the regional averages of $h(err_{f_e})$ and $h(err_{f_t})$ have greater values during the growing season by 0.91 [0.85, 0.98] (mean [95% confidence interval]) and 1.29 [1.06, 1.54] ppm compared to the non-growing season (0.67 [0.63, 0.70] and 1.16 [0.94, 1.37] ppm) because of the tendency for errors in terrestrial biosphere CO_2 fluxes to increase proportionally with the magnitude of flux values. Consequently, transport errors, inferred from the difference between RMSE and $h(err_{f_t})$, are greater in the non-growing season. Given the higher net CO_2 emissions in East Asia during the non-growing season, when terrestrial biosphere CO_2 uptake is less active, this result is consistent with a previous study showing that transport errors are proportional to the magnitude of the net CO_2 flux (Schuh et al., 2019). In addition, we found that the ratio of $h(err_{f_t})$ to $h(err_{f_e})$ is slightly lower during the non-growing season with 0.58 [0.44, 0.72] compared to the growing season with 0.70 [0.53, 0.89], indicating a relatively greater underestimation of true flux errors when the contributions of anthropogenic CO_2 emissions to atmospheric CO_2 changes are higher. This supports our finding that the current inverse model may exhibit a systematic bias related to anthropogenic emissions. Furthermore, the consistent ratio of $h(err_{f_t})$ to $h(err_{f_e})$ below 1, without statistically significant seasonal variations in East Asia, suggests that our conclusions, drawn from the analysis of seven regions, are not seasonally dependent.

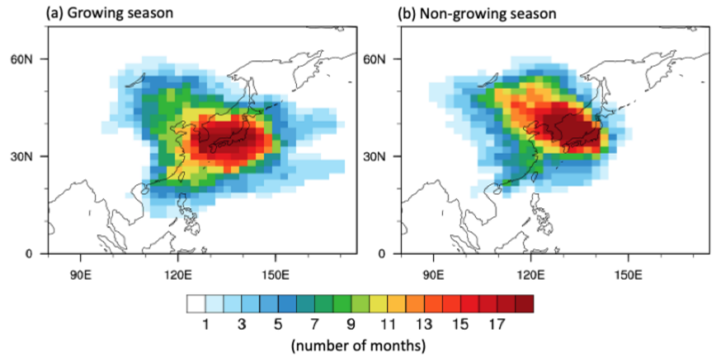

Figure R1 Number of months selected as the effective area for airborne measurements in East Asia during (a) the vegetation growing season and (b) the non-growing season for the period 2015–2017.

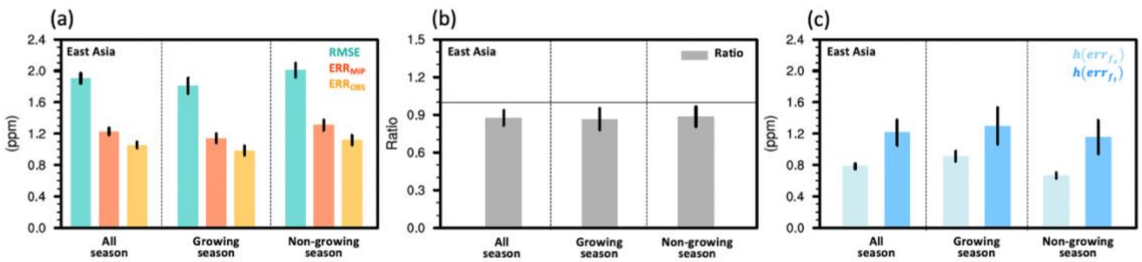

Figure R2 Mean values of monthly (a) RMSE, ERR_{MIP}, ERR_{OBS}, (b) Ratio, (c) $h(err_{f_e})$, and $h(err_{f_t})$ in East Asia during each season for the period 2015–2017. The error bars represent the 95% confidence intervals derived from 1000 bootstrap samples of datasets.

Next, in order to capture the signals from the surface CO_2 fluxes and include as much observation data as possible in our analysis, we used atmospheric CO_2 data observed and simulated within the range of 1-5km altitude (above the ground). To assess the sensitivity of our results to the choice of altitude range, we compared the error quantities derived from atmospheric CO_2 data within two altitude (above the ground) ranges: 1-3 km and 1-5 km. Among the seven analyzed regions, Australia and South America were excluded in this additional analysis due to having fewer than 100 total observed grid points for the analysis period and losing over 30% of the grid points when narrowing the altitude range. This exclusion was necessary as it could substantially alter the areas represented by our error statistics.

The areas sensitive to airborne CO_2 measurements within the two altitude ranges exhibit nearly identical spatial patterns in Alaska, Mid-latitude Norther America, Europe, East Asia, and Southeast Asia, indicating that observations at lower altitudes are more sensitive to surface CO_2 fluxes (Figure R3). Because of the higher sensitivity, error statistics in all regions have larger values when calculated using data from the 1-3 km altitude range compared to the 1-5 km altitude range (Figure R4). For example, in Mid-latitude North America, the regional averages of RMSE, ERR_{TOT}, $h(err_{f_e})$, and $h(err_{f_t})$ are 1.42 [1.35, 1.48], 1.34 [1.30, 1.39], 0.73 [0.70, 0.76], and 0.86 [0.72, 1.00] ppm when calculated using data within the 1-3 km altitude range. In comparison, when computed from the data within the 1-5 km altitude range, these values are 1.20 [1.15, 1.25], 1.09 [1.06, 1.13], 0.58 [0.56, 0.60], and 0.77 [0.66, 0.88] ppm. However, the ratio of $h(err_{f_t})$ to $h(err_{f_e})$, which is a key metric for quantifying the true regional terrestrial biosphere flux error, did not show significant differences based on the altitude ranges, with the difference being between 0.02 and 0.1. Again, these results suggest that our observation-based regional flux error estimates are not sensitive to the choice of altitude range.

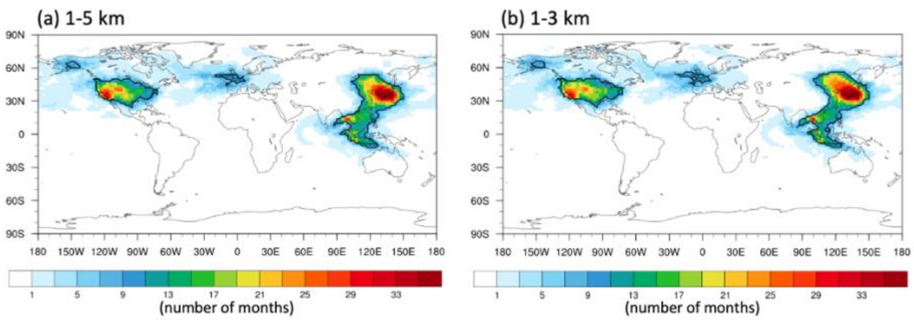

Figure R3 Number of months selected as the effective area for airborne measurements made within (a) the 1-5 km altitude range and (b) 1-3 km altitude range in Alaska, Mid-latitude Norther America, Europe, East Asia, and Southeast Asia for the period 2015–2017. The outlined area represents selected areas for more than eight months or equal.

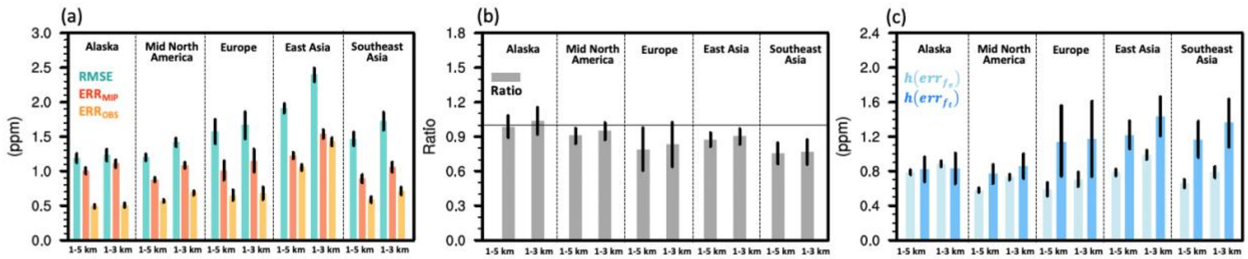

Figure R4 Mean values of monthly (a) RMSE, ERR_{MIP}, ERR_{OBS}, (b) Ratio, (c) $h(err_{f_e})$, and $h(err_{f_t})$ derived from atmospheric CO_2 data within either the 1-5 km or 1-3 km altitude range for each region for the period 2015–2017. The error bars represent the 95% confidence intervals derived from 1000 bootstrap samples of datasets.

We have added Figures R1, R2, R3, and R4 to the revised supplementary information and added the above explanation on the discussion part of the revised manuscript as follow:

"The performance of inverse models in simulating atmospheric CO_2 may vary by season. Airborne measurements were not uniformly conducted across all seasons in most analyzed regions, necessitating an examination of whether the regional averages of error statistics (e.g., Figures 4h, 4i, and 5h) are significantly different with seasons. Among the seven regions analyzed, in East Asia, the Contrail program has continuously conducted CO_2 measurements over three years with routes repeated throughout all seasons. This has resulted in the most sensitive area to the measurements exhibiting similar spatial patterns in the vegetation growing season (from May to October) and non-growing season, encompassing the northeast part of China, the Korean Peninsula, and Japan (Figure S6). The airborne measurements in East Asia offer a unique opportunity to isolate the seasonal impacts on regional error statistics. For the period of 2015–2017, the regional averages of both RMSE and ERR_{TOT} exhibit, on average, 14% and 11% higher values during the non-growing season compared to the growing season (Figure S7). In contrast, the regional averages of $h(err_{f_e})$ and $h(err_{f_t})$ have greater values during the growing season by 0.91 [0.85, 0.98] and 1.29 [1.06, 1.54] ppm compared to the non-growing season (0.67 [0.63, 0.70] and 1.16 [0.94, 1.37] ppm) because of the tendency for errors in terrestrial biosphere CO_2 fluxes to increase proportionally with the magnitude of flux values. Consequently, transport errors, inferred from the difference between RMSE and $h(err_{f_t})$, are greater in the non-growing season. Given the higher net CO_2 emissions in East Asia during the non-growing season, when terrestrial biosphere CO_2 uptake is less active, this result is consistent with a previous study showing that transport errors are proportional to the magnitude of the net CO_2 flux (Schuh et al., 2019). In addition, we found that the ratio of $h(err_{f_t})$ to $h(err_{f_e})$ is slightly lower during the non-growing season with 0.58 [0.44, 0.72] compared to the growing season with 0.70 [0.53, 0.89], indicating a relatively greater underestimation of true flux errors when the contributions of anthropogenic CO_2 emissions to atmospheric CO_2 changes are higher. This supports our finding that the current inverse model may exhibit a systematic bias related to anthropogenic emissions. Furthermore, the consistent ratio of $h(err_{f_t})$ to $h(err_{f_e})$ below 1, without statistically significant seasonal variations in East Asia, indicates that our conclusions, drawn from the analysis of seven regions, are not seasonally dependent.

To capture the signals from surface CO_2 fluxes and maximize observation data in our analysis, we used atmospheric CO_2 data observed and simulated within the 1-5 km altitude range. The choice of altitude range may influence regional error statistics, as the performance of inverse models varies with altitude. To gauge this sensitivity, we compared error statistics derived from atmospheric CO_2 data with two altitude (above the ground) ranges: 1-3 km and 1-5 km. Among the seven analyzed regions, Australia and South America were excluded in this additional analysis due to having fewer than 100 total observed grid points for the analysis period and losing over 30% of the grid points when narrowing the altitude range. The areas sensitive to airborne CO_2 measurements within the two altitude ranges exhibit nearly identical spatial patterns in Alaska, Mid-latitude Norther America, Europe, East Asia, and Southeast Asia, indicating that observations at lower altitudes are more sensitive to surface CO_2 fluxes (Figure S8). Because of the higher sensitivity, error statistics in all regions have larger values when calculated using data from the 1-3 km altitude range compared to the 1-5 km altitude range (Figure S9). For example, in Mid-latitude North America, the regional averages of RMSE, ERR_{TOT}, $h(err_{f_e})$, and $h(err_{f_t})$ are 1.42 [1.35, 1.48], 1.34 [1.30, 1.39], 0.73 [0.70, 0.76], and 0.86 [0.72, 1.00] ppm when calculated using data within the 1-3 km altitude range. In comparison, when computed from the data within the 1-5 km altitude range, these values are 1.20 [1.15, 1.25], 1.09 [1.06, 1.13], 0.58 [0.56, 0.60], and 0.77 [0.66, 0.88] ppm. However, the ratio of $h(err_{f_t})$ to $h(err_{f_e})$, which is a key metric for quantifying the true regional terrestrial biosphere flux error, did not show significant differences based on the altitude ranges, with the difference being between 0.02 and 0.1. Again, these results suggest that our observation-based regional flux error estimates are not sensitive to the choice of altitude range."

3. Lines 124-125: "measurements made between 1 and 5 km altitude" does not specify whether this means above ground level or above sea level. This needs to be specified. Furthermore, if this altitude range is above sea level then it is entirely possible that highly-variable PBL measurement data are included in the evaluation data, since many aircraft data were collected over topography with surface elevations of hundreds of meters ASL. This would cloud the analysis with noisy measurements having strong signals of local exchange.

[Reply] We really appreciate your comment. It turns out that our previous analysis was based on atmospheric CO2 data within the 1-5 km altitude range above sea level, not ground level. We re-calculated all our results using the atmospheric CO_2 data within 1-5 km altitude range "above ground level". The newly computed results, particularly the ratio of RMSE and ERR_{TOT} and the ratio of $h(err_{f_t})$ to $h(err_{f_e})$, key metrics for assessing and quantifying regional terrestrial biosphere flux errors, do not exhibit significant differences compared to the previous results (Table R2).

Table R2 Mean values of the regionally averaged ratios of RMSE to ERR_{TOT} and the ratios of $h(err_{f_t})$ *to* $h(err_{f_e})$ for 2015–2017 with their 95% confidence intervals derived from 1000 bootstrap samples of datasets, calculated using atmospheric CO_2 datasets within the range of 1-5 km altitude above sea level (previous results) or above ground level (revised results).

		Alaska	Mid NA	Europe	East Asia	Southeast Asia	Australia	South America
Previous results	RMSE/ERR_{TOT}	1.04 [0.93, 1.14]	0.90 [0.83, 0.97]	0.79 [0.62, 0.98]	0.84 [0.78, 0.91]	0.75 [0.66, 0.85]	0.76 [0.61, 0.90]	1.01 [0.81, 1.25]
	$h(err_{ft})/h(err_{fe})$	1.07 [0.84, 1.31]	0.73 [0.59, 0.86]	0.52 [0.29, 0.77]	0.59 [0.48, 0.70]	0.56 [0.42, 0.71]	0.61 [0.35, 0.91]	1.03 [0.49, 1.59]
Revised results	RMSE/ERR_{TOT}	**0.98 [0.89, 1.08]**	**0.91 [0.84, 0.97]**	**0.79 [0.61, 0.97]**	**0.87 [0.81, 0.94]**	**0.75 [0.65, 0.86]**	**0.73 [0.59, 0.87]**	**1.03 [0.83, 1.28]**
	$h(err_{ft})/h(err_{fe})$	**0.96 [0.76, 1.17]**	**0.75 [0.61, 0.90]**	**0.52 [0.28, 0.78]**	**0.64 [0.53, 0.77]**	**0.56 [0.41, 0.72]**	**0.59 [0.34, 0.87]**	**1.10 [0.51, 1.79]**

We have clearly addressed that we used atmospheric CO_2 data within 1-5 km altitude range "above ground level" for the analysis in the revised manuscript as follow:

"To minimize the influence of local sources and maximize the influence of regional fluxes, we excluded surface measurements and only considered airborne measurements made between 1 and 5 km altitude **above ground level.**"

4. It is not clear whether the analysis excludes measurements that were assimilated in the LNLGIS experiment. This is a fundamental piece of information needed to understand the analysis and should absolutely be explicitly stated. If assimilation data are included, then the entire analysis needs to be considered differently.

[Reply] In this study, only airborne CO_2 measurement data not assimilated in the LNLGIS experiment were utilized for analysis. We have clearly addressed this in the revised manuscript as follow:

"In addition, only airborne measurement data **not assimilated in the LNLGIS experiment were used** for analysis."

5. The INPE PFP used in this study data have not been screened for water vapor contamination. This is a known problem with PFPs in humid environments and can lead to both a low bias and spurious variability in CO2 measurements. This is a particular concern with tropical aircraft samples due to expected high humidity of sampled air. There are indications that water vapor contamination can persist in PFP flasks so that even dry high-altitude samples may be affected. This water vapor issue in aircraft PFPs has been documented in Baier et al. (2019, https://agupubs.onlinelibrary.wiley.com/doi/10.1029/2019JD031339) and reported at various meetings (e.g. https://gml.noaa.gov/publications/annual_meetings/2019/abstracts/74-190401-B.pdf). As reported to the authors in OCO-2 meetings, about one-third of historical NOAA PFP measurements have been flagged due to suspected water vapor contamination. In the same meetings the authors were cautioned about this issue affecting INPE PFP data. In ObsPack products, INPE PFP data are all flagged as "do not assimilate", indicating that they are neither suitable for assimilation nor for evaluation purposes. Finally, these data are distributed in a special ObsPack product labeled "restricted" in part to warn users about the problem.

[Reply] We appreciate your notification regarding the water vapor contamination issue in the INPE PFP data. We deliberated whether to include this data in our analysis due to the mentioned issue. However, we decided to include it in our analysis because we believe this study can provide valuable insights for future research utilizing bias-corrected observations to quantify biosphere flux errors in South America, one of the most critical regions for terrestrial carbon cycle studies. To ensure that readers are well-informed about this issue before interpreting our results, we have clearly addressed the unresolved water vapor contamination issue of this data and its potential impact on our findings in the revised manuscript as follow:

"This dataset includes five flask measurements provided by the National Institute for Space Research (INPE), which might have a higher measurement error due to water vapor contamination compared to other datasets (Baier et al., 2019). Despite their potential limitation, our analysis, aimed at introducing a method for quantifying flux errors, incorporates INPE data to offer guidance for future studies leveraging bias-corrected observations from this region, is critical for terrestrial carbon cycle studies. Readers should keep in mind that our results from South America may have relatively lower reliability compared to that from other regions."

"However, in reality, systematic errors could be present in airborne observation data stemming from instrument or setup biases, calibration offsets, and other factors. Especially, CO_2 measurements in South America from INPE might exhibit a higher measurement error compared to other regions because of unresolved water vapor contamination issues in the flask measurements, which could result in both a low bias (0.1 and 0.8 ppm at 1.75% and 3–4% absolute humidity, respectively) and spurious variability (Baier et al., 2019). The potential effects of these systematic errors on our findings will be addressed in Section 4."

"First, due to a lack of information, we set observation measurement errors under ideal conditions. In reality, inadequate quality control can result in significant systematic bias for specific regions and time periods (Masarie et al., 2011; Baier et al., 2019), impacting our results, especially in South America. For instance, if this led to an average measurement error of 0.5 ppm during the analysis period, the calculated true flux error would decrease from 351 to 277 TgC year^{-1} for South America and from 371 to 260 TgC year^{-1} for mid-latitude North America."

6. The CO2 measurement data used in this study have not been correctly cited. It also is not clear whether ObsPack data providers have been properly acknowledged. The OCO-2 ObsPack product is a "composite" product created from seven source ObsPacks. The source products need to be cited following the instructions at https://gml.noaa.gov/ccgg/obspack/citation.php (available also in the distributed metadata). Use of an ObsPack product also includes usage terms which suggest that it may be appropriate to offer coauthorship to the data providers. The seven source ObsPacks are listed in the metadata directory of the downloaded product. In the current draft, only the obspack_co2_1_GLOBALVIEWplus_v6.1_2021-03-01 product is cited, whereas apparently there are data used from five other ObsPacks: the NRT product, the Manaus product, the INPE product, the CONTRAIL product, and the AirCore product.

[Reply] We appreciate your guidance for properly acknowledging the ObsPack products. We have included citation information and the DOI for all types of ObsPack data in Table 1 of the revised manuscript (shown in Table R1). The OCO-2 ObsPack products, we used, are originated from following five different Obspack data: obspack_co2_1_GLOBALVIEWplus_v6.1_2021-03-01, obspack_co2_1_AirCore_v4.0_2020-12-28, obspack_co2_1_INPE_RESTRICTED_v2.0_2018-11-13, obspack_co2_1_NRT_v6.1.1_2021-05-17, obspack_multi-species_1_manaus_profiles_v1.0_2021-05-20.

We also reached out to all airborne CO_2 measurement data providers and sought their guidance on proper acknowledgment or co-authorship for utilizing the airborne measurements dataset in this research before submitting this manuscript. During the revision process, SGP flask CO_2 measurement data has been included, leading to the invitation of "Sébastien C. Biraud" as a co-author.

References

1. Baier, B. C., Sweeney, C., Choi, Y., Davis, K. J., DiGangi, J. P., Feng, S., Fried, A., Halliday, H., Higgs, J., Lauvaux, T., Miller, B. R., Montzka, S. A., Newberger, T., Nowak, J. B., Patra, P., Richter, D., Walega, J., and Weibring, P.:

Multispecies Assessment of Factors Influencing Regional CO_2 and CH_4 Enhancements During the Winter 2017 ACT-America Campaign, Journal of Geophysical Research: Atmospheres, 125, e2019JD031339, https://doi.org/10.1029/2019JD031339, 2020.

2. Biraud, S. C., Torn, M. S., Smith, J. R., Sweeney, C., Riley, W. J., and Tans, P. P.: A multi-year record of airborne CO_2 observations in the US Southern Great Plains, Atmospheric Measurement Techniques, 6, 751–763, https://doi.org/10.5194/amt-6-751-2013, 2013.
3. Filges, A., Gerbig, C., Chen, H., Franke, H., Klaus, C., and Jordan, A.: The IAGOS-core greenhouse gas package: a measurement system for continuous airborne observations of CO_2, CH_4, H_2O and CO, Tellus B: Chemical and Physical Meteorology, 67, 27989, https://doi.org/10.3402/tellusb.v67.27989, 2015.
4. Gatti, L. V., Cunha, C. L., Marani, L., Cassol, H. L. G., Messias, C. G., Arai, E., Denning, A. S., Soler, L. S., Almeida, C., Setzer, A., Domingues, L. G., Basso, L. S., Miller, J. B., Gloor, M., Correia, C. S. C., Tejada, G., Neves, R. A. L., Rajao, R., Nunes, F., Filho, B. S. S., Schmitt, J., Nobre, C., Corrêa, S. M., Sanches, A. H., Aragão, L. E. O. C., Anderson, L., Von Randow, C., Crispim, S. P., Silva, F. M., and Machado, G. B. M.: Increased Amazon carbon emissions mainly from decline in law enforcement, Nature, 621, 318–323, https://doi.org/10.1038/s41586-023-06390-0, 2023.
5. Karion, A., Sweeney, C., Tans, P., and Newberger, T.: AirCore: An Innovative Atmospheric Sampling System, Journal of Atmospheric and Oceanic Technology, 27, 1839–1853, https://doi.org/10.1175/2010JTECHA1448.1, 2010.
6. Kawa, S. R., Abshire, J. B., Baker, D. F., Browell, E. V., Crisp, D., Crowell, S. M. R., Hyon, J. J., Jacob, J. C., Jucks, K. W., Lin, B., Menzies, R. T., and Ott, L. E., and Zaccheo, T. S.: Active Sensing of CO_2 Emissions over Nights, Days, and Seasons (ASCENDS): Final Report of the ASCENDS Ad Hoc Science Definition Team, Document ID: 20190000855, NASA/TP–2018-219034, GSFC-E-DAA-TN64573, 2018.
7. Machida, T., Matsueda, H., Sawa, Y., Nakagawa, Y., Hirotani, K., Kondo, N., Goto, K., Nakazawa, T., Ishikawa, K., and Ogawa, T.: Worldwide Measurements of Atmospheric CO_2 and Other Trace Gas Species Using Commercial Airlines, Journal of Atmospheric and Oceanic Technology, 25, 1744–1754, https://doi.org/10.1175/2008JTECHA1082.1, 2008.
8. Miller, J. B., Martins, G. A., de Souza, R. A., and Schuldt, K. N.: Manaus Aircraft profile data for the period 2017-2020; obspack_multi-species_1_manaus_profiles_v1.0_202105-19, NOAA Global Monitoring Laboratory [data set], https://doi.org/10.25925/20210519, 2021.
9. NOAA Carbon Cycle Group ObsPack Team; (2018): INPE atmospheric carbon dioxide data for the period 2015-2017; obspack_co2_1_INPE_RESTRICTED_v2.0_2018-11-13; NOAA Earth System Research Laboratory, Global Monitoring Division. http://dx.doi.org/10.25925/20181030.
10. Schuh, A. E., Jacobson, A. R., Basu, S., Weir, B., Baker, D., Bowman, K., Chevallier, F., Crowell, S., Davis, K. J., Deng, F., Denning, S., Feng, L., Jones, D., Liu, J., and Palmer, P. I.: Quantifying the Impact of Atmospheric Transport Uncertainty on CO_2 Surface Flux Estimates, Global Biogeochemical Cycles, 33, 484–500, https://doi.org/10.1029/2018GB006086, 2019.
11. Schuldt, K. N., Jacobson, A. R., Aalto, T., Andrews, A., Bakwin, P., Bergamaschi, P., Biermann, T., Biraud, S. C., Chen, H., Colomb, A., Conil, S., Cristofanelli, P., De Mazière, M., De Wekker, S., Delmotte, M., Dlugokencky, E., Emmenegger, L., Fischer, M. L., Hatakka, J., Heliasz, M., Hermanssen, O., Holst, J., Jaffe, D., Karion, A., Kazan, V., Keronen, P., Kominkova, K., Kubistin, D., Laurent, O., Laurila, T., Lee, J., Lehner, I., Leuenberger, M., Lindauer, M., Lopez, M., Mammarella, I., Manca, G., Marek, M. V., McKain, K., Miller, J. B., Miller, C. E., Myhre, C. L., Mölder, M., Müller-Williams, J., Piacentino, S., Pichon, J. M., Plass-Duelmer, C., Ramonet, M., Scheeren, B., Schumacher, M., Sha, M. K., Sloop, C. D., Smith, P., Steinbacher, M., Sweeney, C., Tans, P., Thoning, K., Trisolino, P., Tørseth, K., Viner, B., Vitkova, G., and di Sarra, A. G.: Multi-laboratory compilation of atmospheric carbon dioxide data for the years 2020–2021;

obspack_co2_1_NRT_v6.1.1_2021-05-17, NOAA Earth System Research Laboratory, Global Monitoring Laboratory [data set], https://doi.org/10.25925/20210517, 2021a.

12. Schuldt, K. N., Mund, J., Luijkx, I. T., Aalto, T., Abshire, J. B., Aikin, K., Andrews, A., Aoki, S., Apadula, F., Baier, B., Bakwin, P., Bartyzel, J., Bentz, G., Bergamaschi, P., Beyersdorf, A., Biermann, T., Biraud, S. C., Boenisch, H., Bowling, D., Brailsford, G., Chen, G., Chen, H., Chmura, L., Clark, S., Climadat, S., Colomb, A., Commane, R., Conil, S., Cox, A., Cristofanelli, P., Cuevas, E., Curcoll, R., Daube, B., Davis, K., Mazière, M. D., De Wekker, S., Della Coletta, J., Delmotte, M., DiGangi, J. P., Dlugokencky, E., Elkins, J. W., Emmenegger, L., Fang, S., Fischer, M. L., Forster, G., Frumau, A., Galkowski, M., Gatti, L. V., Gehrlein, T., Gerbig, C., Gheusi, F., Gloor, E., Gomez-Trueba, V., Goto, D., Griffis, T., Hammer, S., Hanson, C., Haszpra, L., Hatakka, J., Heimann, M., Heliasz, M., Hensen, A., Hermanssen, O., Hintsa, E., Holst, J., Jaffe, D., Joubert, W., Karion, A., Kawa, S. R., Kazan, V., Keeling, R., Keronen, P., Kolari, P., Kominkova, K., Kort, E., Kozlova, E., Krummel, P., Kubistin, D., Labuschagne, C., Lam, D. H., Langenfelds, R., Laurent, O., Laurila, T., Lauvaux, T., Law, B., Lee, O. S., Lee, J., Lehner, I., Leppert, R., Leuenberger, M., Levin, I., Levula, J., Lin, J., Lindauer, M., Loh, Z., Lopez, M., Machida, T., Mammarella, I., Manca, G., Manning, A., Manning, A., Marek, M. V., Martin, M. Y., Matsueda, H., McKain, K., Meijer, H., Meinhardt, F., Merchant, L., Mihalopoulos, N., Miles, N., Miller, C. E., Miller, J. B., Mitchell, L., Montzka, S., Moore, F., Morgan, E., Morgui, J.-A., Morimoto, S., Munger, B., Myhre, C. L., Mölder, M., Obersteiner, F., M uller-Williams, J., Necki, J., Newman, S., Nichol, S., Niwa, Y., O'Doherty, S., Paplawsky, B., Peischl, J., Peltola, O., Pichon, J. M., Piper, S., Plass-Duelmer, C., Ramonet, M., Ramos, R., Reyes-Sanchez, E., Richardson, S., Riris, H., Rivas, P. P., Ryerson, T., Saito, K., Sargent, M., Sasakawa, M., Sawa, Y., Say, D., Scheeren, B., Schuck, T., Schumacher, M., Seifert, T., Sha, M. K., Shepson, P., Shook, M., Sloop, C. D., Smith, P., Steinbacher, M., Stephens, B., Sweeney, C., Tans, P., Thoning, K., Timas, H., Torn, M., Trisolino, P., Turnbull, J., Tørseth, K., Vermeulen, A., Viner, B., Vitkova, G., Walker, S., Watson, A., Wofsy, S., Worsey, J., Worthy, D., Young, D., Zahn, A., Zimnoch, M., van Dinther, D., and van den Bulk, P.: Multi-laboratory compilation of atmospheric carbon dioxide data for the period 1957–2019; obspack_co2_1_GLOBALVIEWplus_v6.1_2021-03-01, NOAA Earth System Research Laboratory, Global Monitoring Laboratory [data set], https://doi.org/10.25925/20201204, 2021b.
13. Stephens, B. B., Long, M. C., Keeling, R. F., Kort, E. A., Sweeney, C., Apel, E. C., Atlas, E. L., Beaton, S., Bent, J. D., Blake, N. J., Bresch, J. F., Casey, J., Daube, B. C., Diao, M., Diaz, E., Dierssen, H., Donets, V., Gao, B.-C., Gierach, M., Green, R., Haag, J., Hayman, M., Hills, A. J., Hoecker-Martínez, M. S., Honomichl, S. B., Hornbrook, R. S., Jensen, J. B., Li, R.-R., McCubbin, I., McKain, K., Morgan, E. J., Nolte, S., Powers, J. G., Rainwater, B., Randolph, K., Reeves, M., Schauffler, S. M., Smith, K., Smith, M., Stith, J., Stossmeister, G., Toohey, D. W., and Watt, A. S.: The O_2/N_2 Ratio and CO_2 Airborne Southern Ocean Study, Bulletin of the American Meteorological Society, 99, 381–402, https://doi.org/10.1175/BAMS-D-16-0206.1, 2018.
14. Sweeney, C., Karion, A., Wolter, S., Newberger, T., Guenther, D., Higgs, J. A., Andrews, A. E., Lang, P. M., Neff, D., Dlugokencky, E., Miller, J. B., Montzka, S. A., Miller, B. R., Masarie, K. A., Biraud, S. C., Novelli, P. C., Crotwell, M., Crotwell, A. M., Thoning, K., and Tans, P. P.: Seasonal climatology of CO_2 across North America from aircraft measurements in the NOAA/ESRL Global Greenhouse Gas Reference Network, Journal of Geophysical Research: Atmospheres, 120, 5155–5190, https://doi.org/10.1002/2014JD022591, 2015.
15. Weir, B., Crisp, D., O'Dell, C. W., Basu, S., Chatterjee, A., Kolassa, J., Oda, T., Pawson, S., Poulter, B., Zhang, Z., Ciais, P., Davis, S. J., Liu, Z., and Ott, L. E.: Regional impacts of COVID-19 on carbon dioxide detected worldwide from space, Science Advances, 7, eabf9415, https://doi.org/10.1126/sciadv.abf9415, 2021.